Space and time dynamical heterogeneity in glassy relaxation. The role of democratic clusters

TOPICAL REVIEW

Space and time dynamical heterogeneity in glassy relaxation. The role of democratic clusters

G A Appignanesi and J A Rodriguez Fris

Fisicoquímica, Departamento de Química, Universidad Nacional del Sur, Avenida Alem 1253, 8000 Bahía Blanca, Argentina
and
Sección de Fisicoquímica, Instituto de Química de la Universidad Nacional del Sur, INQUISUR-UNS-CONICET, Universidad Nacional del Sur, Avenida Alem 1253, 8000 Bahía Blanca, Argentina

E-mail: appignan@criba.edu.ar

Abstract
In this work we review recent computational advances in the understanding of the relaxation dynamics of supercooled glass-forming liquids. In such a supercooled regime these systems experience a striking dynamical slowing down which can be rationalized in terms of the picture of dynamical heterogeneities, wherein the dynamics can vary by orders of magnitude from one region of the sample to another and where the sizes and timescales of such slowly relaxing regions are expected to increase considerably as the temperature is decreased. We shall focus on the relaxation events at a microscopic level and describe the finding of the collective motions of particles responsible for the dynamical heterogeneities. In so doing, we shall demonstrate that the dynamics in different regions of the system is not only heterogeneous *in space* but also *in time*. In particular, we shall be interested in the events relevant to the long-time structural relaxation or α relaxation. In this regard, we shall focus on the discovery of cooperatively relaxing units involving the collective motion of relatively compact clusters of particles, called 'democratic clusters' or d-clusters. These events have been shown to trigger transitions between metabasins of the potential energy landscape (collections of similar configurations or structures) and to consist of the main steps in the α relaxation. Such events emerge in systems quite different in nature such as simple model glass formers and supercooled amorphous water. Additionally, another relevant issue in this context consists in the determination of a link between structure and dynamics. In this context, we describe the relationship between the d-cluster events and the constraints that the local structure poses on the relaxation dynamics, thus revealing their role in reformulating structural constraints.

Contents

1. Introduction

Many liquids, when cooled below their melting temperature fast enough to prevent crystallization, enter a metastable (supercooled) regime [1–8]. If one continues cooling, such systems will eventually form a glass (an amorphous solid that lacks the periodical long-range order of a crystal) at a temperature called the glass-transition temperature T_g [1–8]. When one measures the behaviour of the dynamical properties of such a glass-forming system in the supercooled regime (like the viscosity, the diffusion constant or the relaxation time) it is found that they display a strong temperature dependence (at variance from the structural or thermodynamic observables that only show mild changes when the temperature is altered)[1] [1–8]. In fact, in this regime the liquid suffers a dramatic slowing down of its dynamics within a narrow temperature range [1–8]. The reasons for the emergence of this dynamical slowing down are still poorly understood and represent a major challenge in condensed matter. It is expected that such a strong temperature dependence of the relaxation of the system should arise from a non-trivial microscopic dynamics. This is indeed the case since supercooled liquids have been shown (both experimentally [9–11] and computationally [12–14]) to be dynamically heterogeneous with different regions of the system presenting dynamics that vary from each other even by orders of magnitude. Thus, it becomes central to determine how the individual movements of the particles (including possible cooperative motions or other mechanisms) determine the emergence of the slow relaxation in the system. Computer simulations have proven particularly apt to this end [15], since the dynamics of a relatively large number of particles can be followed for times relatively long, thus providing fully detailed access to microscopic structural and dynamical information, and exhaustive studies both for model and realistic glass formers have been performed. The present review is devoted to present some of the recent computational progress in this field that has helped to shed some light on this issue. For space reasons we shall not include a description of the different very interesting theoretical and computational approaches to the subject, some of which can be found in the following reference list [16–25]. Rather, we have chosen to emphasize here some advances that lie within the dynamical heterogeneity scenario, and particularly, that in which we have been mainly involved. For more complete and comprehensive treatments of the subject, please refer, for example, to some recent, good reviews [26, 15, 8, 27, 28, 11] and references therein.

2. Model system

Even when we shall also refer to other systems (such as SPC/E (simple point charge extended model) water, for instance), most of the results we shall show come from molecular dynamic (MD) NVE (microcanonical ensemble: constant number of particles, volume and energy) simulations for an archetypical model glass former: the binary Lennard-Jones system of Kob and Andersen [15, 29–31]. Thus, we here briefly describe such a system: it consists of

a three-dimensional (3D) mixture of 80% A and 20% B particles, the size of the A particles being larger than the B ones [15, 12, 13, 32][2]. The interaction between two particles of type α and β is given by $V_{\alpha\beta}(r) = 4\epsilon_{\alpha\beta}\{(\sigma_{\alpha\beta}/r)^{12} - (\sigma_{\alpha\beta}/r)^6\}$, where r is the distance between the centres of particle α and particle β; $\alpha, \beta \in \{A, B\}$. The parameters used are $\epsilon_{AA} = 1.0$, $\sigma_{AA} = 1.0$, $\epsilon_{AB} = 1.5$, $\sigma_{AB} = 0.8$, $\epsilon_{BB} = 0.5$, and $\sigma_{BB} = 0.88$. These interactions have been truncated and shifted at $r_{cutoff} = 2.5\sigma_{\alpha\beta}$. In the following we will use σ_{AA} and ϵ_{AA} as units of length and energy, respectively, and measure time in units of $(m\sigma_{AA}^2/48\epsilon_{AA})^{1/2}$ ($m = 1$). The equations of motion were solved for the NVE ensemble at a particle density of 1.2, using the velocity form of the Verlet algorithm with a time step of 0.02. All the presented results correspond to the situation in equilibrium. The mode-coupling temperature for this system has been estimated in $T_c = 0.435$. This T_c is located in the bend of a semilogarithmic plot of the viscosity against reciprocal temperature [5, 34]. We mention that this simple non-realistic system shows a dynamical behaviour consistent with that expected for a glass former and many of the results we shall review here have also been found in more realistic models (as SPC/E supercooled water).

3. Dynamical heterogeneities in glass formers

One of the simplest time-dependent correlation functions to focus on when studying the dynamics of a glass former is the mean squared displacement function:

$$\langle r^2(t) \rangle = \frac{1}{N} \sum_{i=1}^{N} |\mathbf{r}_i(t) - \mathbf{r}_i(0)|^2,$$

where $\mathbf{r}_i(t)$ is the position of particle i at time t, N is the number of particles and $\langle \cdots \rangle$ is the average over different starting times. Figure 1 shows the typical outcome of the computation of this function for the above-mentioned binary Lennard-Jones system at $T = 0.50$. As typical for low temperatures close to T_c (see figure 1), the function shows at first a ballistic regime (slope 2) and then a plateau, followed by the typical diffusive regime (slope 1). The ballistic or inertial regime at very short times corresponds to the short-time movements of the particles before being 'aware' of the confinement to which they are subject by their first neighbours (before colliding to a wall of such cage). The plateau, in turn, emerges from the impossibility at short times to abandon such a cage, while the diffusive regime sets in only when the particles have been able to escape. At high temperatures there is no presence of the plateau displayed in figure 1, but as T decreases (albeit in a narrow T range, say between $T \approx 0.6$ and T_c), the timescale for the caging regime increases considerably, thus signalling the dynamical slowing down. The diffusive regime contains the α (or structural) relaxation timescale τ_α (see figure 1), which marks the decay of the self-intermediate scattering function and which can be well fitted by the ubiquitous non-Debye stretched exponential Kohlrausch relaxation law [15].

---

[1] Silica (SiO_2) also shows this behaviour in the liquid (not supercooled) state.
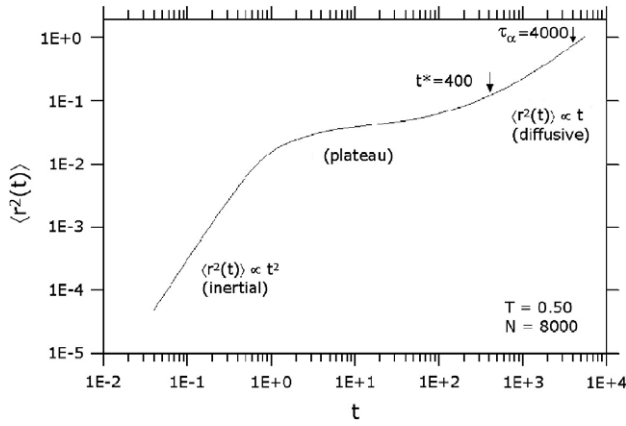
[2] We use reduced units as in [32].

Figure 1. For the binary Lennard-Jones system of $N = 8000$ at $T = 0.50$: the mean squared displacement function, the timescale of maximum inhomogeneous dynamical behaviour t^* and the structural relaxation time τ_α.

Figure 2. Cluster of mobile particles for the binary Lennard-Jones system with $N = 8000$ at $T = 0.50$. The fraction of mobile particles is 6.4%. In white we denote the positions occupied by the mobile particles at $t = 0$ while their positions at time t^* are given by the grey spheres.

If the trajectories of the particles were Gaussian, the so-called 'non-Gaussian parameter' [33], $\alpha_2(t) = [3\langle r^4(t)\rangle]/[(5\langle r^2(t)\rangle^2)] - 1$, would vanish ($r^n(t)$ is the average of the n-moment displacement of the particles at time t). This is indeed the case at high temperatures. However, at low temperatures the non-Gaussian parameter displays non-trivial features. At short and long times, such a parameter presents negligible values since the behaviour is ballistic (thus Gaussian) and diffusive (also Gaussian) respectively, but at intermediate times it presents a maximum, whose height increases and moves to larger times as T decreases. This timescale of maximum inhomogeneous behaviour, the time for the maximum in the curve which is called t^*, is located at the end of the plateau-beginning of the diffusive regime in the $\langle r^2(t)\rangle$ curve (see figure 1). To link this behaviour to the motion of the individual particles, the self part of the van Hove function (for an isotropic system, where the data do not depend on displacement direction but on displacement modulus r) $4\pi r^2 G_s(r, t^*)$ has been analysed at such a timescale t^*. This function gives the probability for a particle to be located after time t^* at distance r from the position it occupied originally at time $t = 0$ and is given by [34]:

$$4\pi r^2 G_s(r, t^*) = \frac{1}{N} \frac{1}{dr} \sum_{i=1}^{N} \left\langle \int_{r-\frac{dr}{2}}^{r+\frac{dr}{2}} \delta(r - |\mathbf{r}_i(t^*) - \mathbf{r}_i(0)|) \, dr \right\rangle,$$

where δ is the Dirac delta 'function'. At low temperatures, if the function $4\pi r^2 G_s(r, t^*)$ is evaluated for the A particles and compared to the curve of $4\pi r^2 G^0(r, t^*)$ (the self part of the van Hove function of the corresponding Gaussian process) it can be learnt that $4\pi r^2 G_s(r, t^*)$ presents a long tail that exceeds $4\pi r^2 G^0(r, t^*)$. Thus, this means that some particles are moving faster than would be expected for a Gaussian movement. The value of such intersection r^* between $4\pi r^2 G_s(r, t^*)$ and $4\pi r^2 G^0(r, t^*)$ was defined as a criterion to indicate 'mobile' particles [12]. For $T = 0.50$ this value is around 0.6 (a value that does not change much for
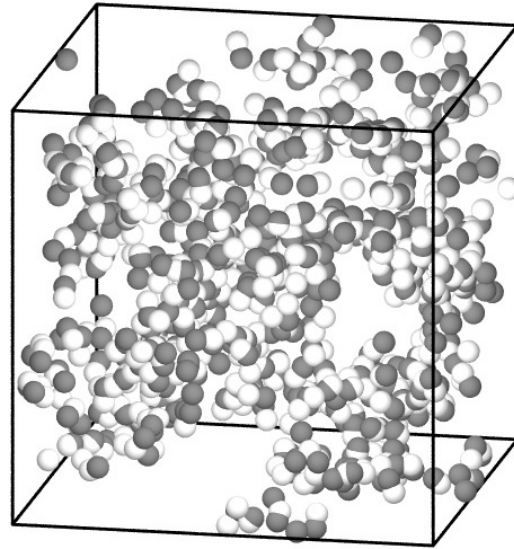
temperatures not too different) and it was found that around 5%–10% of the particles moved more than r^* (a very similar percentage was also found for other close temperatures above T_c). The important point is that when looking for the spatial distribution of such mobile particles, it was found that they were not homogeneously distributed in the sample, but that they were arranged in clusters (as can be seen in figure 2 for an example taken from the same run of our system of $N = 8000$ of figure 1). These clusters were in turn made up by string-like clusters in the sense that the mobile particles tended to replace their neighbours within a certain distance after t^* [13, 14] (for $T = 0.50$ the string criterion was that a step of the string involving two particles i and j implied that the distance between the position of particle j at time t^* and the position of particle i at time $t = 0$ was less than 0.6; however, this value did not change much for other close temperatures). These cooperative string-like motions received experimental confirmation by the work of Weeks *et al* and Kegel *et al* who used confocal microscopy to track the motion of individual particles in a glass former consisting of a dense colloidal suspension [35, 36]. However, a detailed analysis of the molecular dynamics computer simulations demonstrated that a cluster like that of figure 2 is not the outcome of a single event but instead is the result of many different (string) motions of particles that occur asynchronically [37, 38]. That is, fast string motions in different regions of the system occur at different times within the t^* time span, thus building up the global cluster of mobility. In turn, large string-like clusters also decompose in sub-string motions that occur at different times, and whose displacement has been shown to be of ballistic nature [38].

It is interesting to remember that more than 40 years ago Adam and Gibbs proposed a theory for the relaxation dynamics of glass-forming liquids in which the relaxation was triggered

by 'cooperatively rearranging regions' (CRR) which undergo a spontaneous relaxation [18]. As T diminishes the size of the CRRs should increase as well as their relaxation time, as an increasing number of particles would be demanded, with the concurrent loss in configurational entropy.

4. Finding 'democratic' clusters

The above-expounded results demonstrated the existence of dynamical heterogeneities in glass-forming systems. However, they provided no response to the question of which events should be held responsible for the long-time structural relaxation of the system (the α relaxation). They were also unable to determine whether the dynamics (clearly heterogeneous in space) was also heterogeneous or homogeneous *in time*. Since at any given instant a large system presents some strings (given the fact that string motions occur at different times in different parts of the system), the dynamics averaged over a macroscopically large system would look homogeneous in time (the $\langle r^2(t)\rangle$ function is invariant regarding the choice of the time origin). However, at short enough length scales compatible to the size of the supposed differently (cooperatively) relaxing regions, there is no reason to expect the dynamics to be homogeneous in time, as evidenced by the above-expounded studies of the time development of string motions [37, 38]. Thus, a main question is whether the α relaxation is a gradual process or whether there exist dynamical events particularly responsible for such structural relaxation. And since the size of the relaxing regions and their timescales are expected to grow as T decreases (in fact, the mean size of the strings increases on lowering T towards T_c [13]), this question is of particular interest regarding the nature of the glass transition. Thus, it was obvious to focus on small systems and so, in [32], systems of $N = 150$ particles at $T = 0.50$ were used[3]. Here we shall present the results for an isolated small system of $N = 150$ [32] but later on we shall also take another approach by dividing a large $N = 8000$ system into 64 equal-size cubic boxes of around 125 particles each (we shall label the particles of each box and follow the dynamic of the corresponding particles for a timescale of length τ_α). A useful quantity to investigate the dynamics of the small systems is the 'distance matrix' $\Delta^2(t', t'')$ [39, 32], a quantity that contains information as to what extent a configuration at time t'' is correlated to a configuration at time t':

$$\Delta^2(t', t'') = \frac{1}{N_{\text{box}}} \sum_{i=1}^{N_{\text{box}}} |\mathbf{r}_i(t') - \mathbf{r}_i(t'')|^2,$$

where N_{box} is the number of particles within the box (for the isolated system of $N = 150$ particles $N_{\text{box}} = 150$, but for subsystems within the system of $N = 8000$, N_{box} would be around 125). Note that although *on average* such a correlation will depend only on the time difference $|t'' - t'|$ for large

---

[3] We wish to note that it has been found that the dynamics of small systems of around a hundred particles and that of larger systems of around $N = 8000$ do not differ much, thus these small system sizes do not present important finite size effects [47, 49, 32].
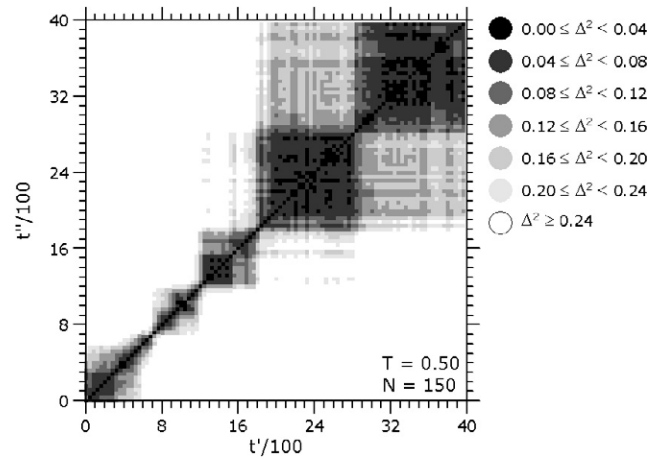

Figure 3. Typical contour plot of the distance matrix $\Delta^2(t', t'')$ for $T = 0.50$ for an isolated small $N = 150$ system. The grey levels correspond to the values that are given to the right. Adapted from [32].

systems (see figure 11), in general Δ^2 will indeed depend on both time arguments, *if the system size is small* (see figure 3).

For high temperatures a contour plot of Δ^2 as a function of t' and t'' shows a narrow dark region along the main diagonal which quickly fades out as one moves away from such a diagonal (for t' very different from t''). This means that the trajectory of the system behaves homogeneously in time and visits configurations that are structurally very different at each time. However, at low temperatures the pattern is completely different, as can be seen in figure 3 where we show the t' and t'' dependence of Δ^2 for a system at $T = 0.50$ and where clear sharply delimited square islands can be seen. This means that the trajectory of the system is most of the time confined to groups of structurally similar closely related configurations (it is confined to certain regions of configuration space, the square islands in the distance matrix) and sporadically suffers rapid crossings between such regions. While the configurations within a given group (within an square island) are mutually similar, they are structurally different from the ones of other regions (the other square islands).

Here we have used the instantaneous configurations (the so-called real dynamics). However, the physical meaning of figure 3 acquires additional content within the vastly used 'energy landscape' approach (in fact, the potential energy landscape, see, e.g. [3, 40, 41] for a more extensive discussion), which we shall hereby sketch. Rooted on the early ideas of Goldstein [42], this approach is based on the fact that the potential energy of the system as a function of the coordinates of all the comprising particles is a complex hypersurface with many minima separated from others by energy barriers. Stillinger and coworkers [43–46] associated to each configuration of particles the so-called 'inherent structure' (IS), the local minimum in the potential energy that is found when the configuration of interest is subject to a steepest descent procedure. This mapping method decomposes the potential energy landscape into a set of IS (basins of attraction, for all the real structures that have the same IS [47]). Thus, at low enough temperatures the dynamics of the system

can be considered as a collection of jumps from one IS to a neighbouring one, followed by an equilibration within the local IS. Additionally, the hierarchical organization of the landscape of glass formers in metabasins (MB) has been postulated and detected, while the transition between MBs has been proposed to be related to the α relaxation [45, 3, 47] (thus an MB would be a group of ISs separated from each other by low barriers, while large barriers would separate neighbouring MBs). In turn, the average sojourn time of the binary Lennard-Jones system of interest in an IS is quite small, much smaller than the timescale t^* [47]. Thus, in this language, the dark islands of figure 3 represent a clear indication of the MB arrangement of the energy landscape. Typical sojourn times of the system in an MB at $T = 0.50$ are (in time units) 300–800, which corresponds to about 10%–20% of the α-relaxation time τ_α, which is 4000 time units [32]. This implies that within such a region the system makes many jumps between local minima but, since the distance matrix Δ^2 is not increasing, these jumps do not really help to propagate the system in configuration space, a task which is instead performed by the crossings between the MBs.

It is worth noting that for lower temperatures the behaviour of the system is similar to that already described, but that the sojourn time of the system within one MB increases rapidly (in the same trend as that of the increment of τ_α). On the contrary, as already indicated, a temperature increase basically washes out the MB structure since the barriers between consecutive MBs can be easily overcome. We also indicate that qualitatively similar results have been obtained by a direct investigation of the ISs by an interval bisection method, an approach which is, however, much more costly in terms of computer resources [47–49]. Also, besides its simplicity as compared to other methods, the advantage of the distance matrix technique is that it makes it possible to study portions of any size from a large system since it relies only on particle coordinates and not on potential energy. This has also the benefit that for systems of arbitrarily small size there is no need to modify the original potential of the Kob–Andersen model, as demanded by other methods. Here we have used the instantaneous real configurations to build the distance matrix. If we had instead used the corresponding ISs, the resulting plot would have been almost identical (however, we shall not pursue here the discussion of the description of the MB structure of the landscape beyond these qualitative terms, since a deep quantitative description has been provided by [47–49] and there is already an excellent review on the subject [26]).

In figure 4 we show for the same run (and same time interval) $\delta^2(t, \theta)$, the (particle) average squared displacement of the particles within a time interval θ (solid line, right scale). This function is defined as [32]:

$$\delta^2(t, \theta) = \Delta^2(t - \theta/2, t + \theta/2)$$
$$= \frac{1}{N_{\text{box}}} \sum_{i=1}^{N_{\text{box}}} |\mathbf{r}_i(t - \theta/2) - \mathbf{r}_i(t + \theta/2)|^2.$$

Thus $\delta^2(t, \theta)$ is $\Delta^2(t', t'')$ measured along the diagonal $t'' = t' + \theta$ and hence the average of this quantity over different starting times t gives the usual mean squared displacement for
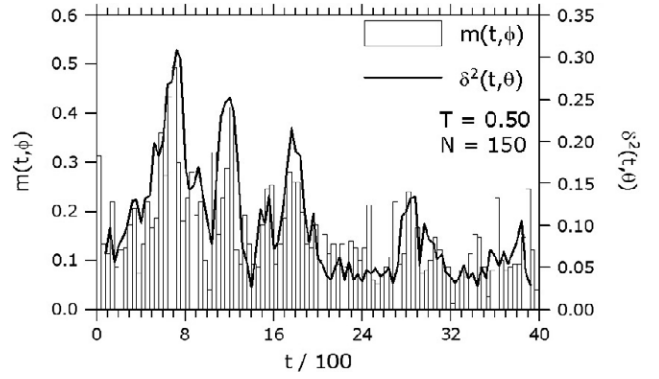

Figure 4. Solid line (right scale): average squared displacement $\delta^2(t, \theta)$, for the trajectory given in figure 3. The value of θ is 160. Vertical bars (left scale): the function $m(t, \phi)$ which gives the fraction of democratic particles, i.e. particles that moved more than the threshold value $r_{\text{th}} = 0.3$ in the time interval $[t - \phi/2, t + \phi/2]$, using $\phi = 40$. Adapted from [32].

time lag θ, that is $\langle r^2(\theta) \rangle$. For this plot we have chosen $\theta = 160$, a value that is significantly smaller than the α-relaxation time $\tau_\alpha (=4000)$ but still sufficiently larger than the time of the microscopic vibrations $(=O(1))$. We can easily note that the δ^2 curve shows important peaks exactly when the system leaves an MB (escaping from a dark square-like island of the contour plot of the distance matrix). Thus, each transition between two neighbouring MBs, or simply an MB–MB transition, is indeed associated with a rapid (average) motion of the system as measured by δ^2.

To further evidence the role of particle movements in the MB–MB transition events, we have calculated $4\pi r^2 G'_s(r, t, \phi)$ [32], the (normalized) distribution of the displacements r of the particles for a given time interval of length $\phi = 40$ (note that the average of $4\pi r^2 G'_s(r, t, \phi)$ over t gives $4\pi r^2 G_s(r, \phi)$). This distribution is shown in figure 5(a) for values of t that correspond to times at which δ^2 shows a plateau, i.e. when the system is exploring an MB. Also included in the graph is the self part of the van Hove function $4\pi r^2 G_s(r, \phi)$. We can see that both distributions are virtually indistinguishable, thus indicating that while the trajectory is confined within an MB the system moves basically as on average. In figure 5(b) we show the same distributions but now calculated at times when the system is about to leave an MB (as can be learnt by comparing with the boundaries of the square islands of the distance matrix). Notably, the distributions are displaced to the right with respect to $4\pi r^2 G_s(r, \phi)$, showing a clear enhancement in the movements of the particles. Since there is no preference in the displacements for large motions (all kinds of displacements are possible) we conclude that the rapid increase of δ^2 is *not* due to the presence of a *few* very-mobile particles, but instead to what we called [32] a 'democratic' movement of *many* particles (many of them not performing very large displacements). This finding is contrary to the results of the cooperative string-like motion on the timescale of t^* which implied the very large movements (close to the interparticle distance) of a few particles (5%–10% of the sample) [12, 13, 36, 35].
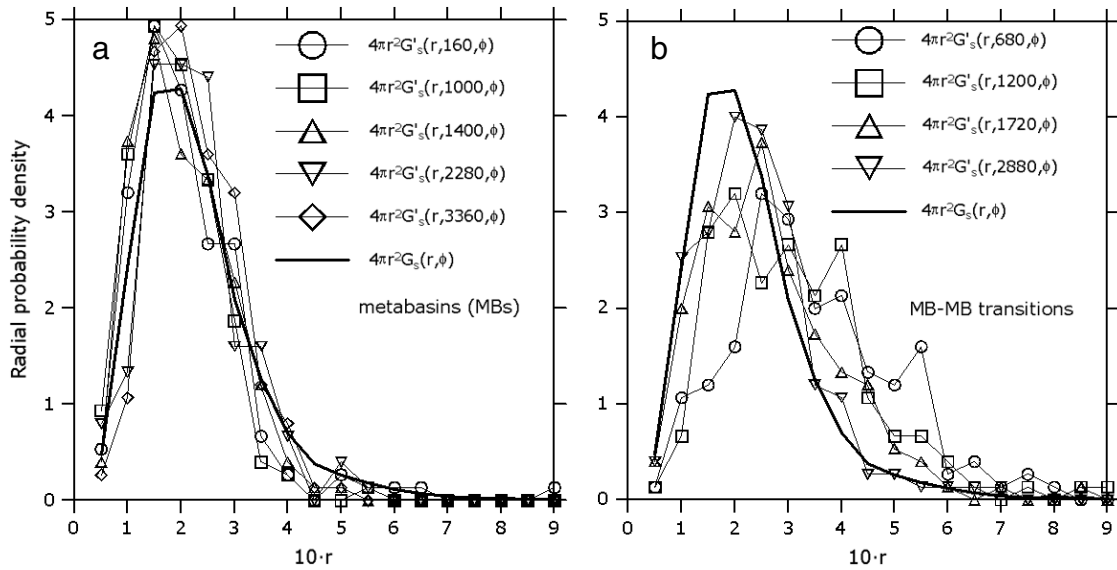
Figure 5. Normalized displacement distribution functions for the binary Lennard-Jones system with parameters $N = 150$ and $T = 0.50$. Curves with symbols: r (displacement) dependence of the function $4\pi r^2 G'_s(r, t, \phi)$. The value of ϕ is 40. The bold curve is $4\pi r^2 G_s(r, \phi)$, the self part of the van Hove function. (a) Values of t in which the system is inside an MB. (b) Values of t for which the system is about to leave an MB. Adapted from [32].

To demonstrate that these motions involve a substantial number of particles and that they are strongly correlated with peaks in δ^2, we have defined as 'democratic' all those particles that in the time interval $\phi = 40$ have moved more than $r_{th} = 0.3$, and denote the fraction of such particles by $m(t, \phi)$ [32]. That this is precisely the case can be seen in figure 4 (vertical bars, left scale). The fraction of democratic particles is of the order of 30%–40% of the system and thus significantly larger than one would expect from $4\pi r^2 G_s(r, \phi)$ if one integrates this distribution from r_{th} to infinity (which gives around 0.15, or 15% since the area under the whole curve is 1). Thus, in contrast to the string situation, the events relevant to the α relaxation of the region considered involve a substantial number of particles and not just a few.

The results of figures 4 and 5(b) demonstrate that MB–MB transitions entail a significant increase in the mobility of the system. An obvious question is whether such democratic particles are located at random in the simulation box or if they are clustered, as was the case for the previous motions identified in the context of dynamical heterogeneities. Figure 6 shows a typical spatial distribution in the simulation box of democratic particles before such an MB–MB transition event. Each particle has an arrow attached indicating its position after the event, i.e. a time $\phi = 40$ later. From this graph it becomes evident that the MB–MB transitions correspond to a movement in which the particles form a relatively compact cluster. This relatively compact nature is at variance with the situation in the string-like motions [13, 37, 38] which is non-compact. Such relatively compact regions (termed as 'democratic clusters' or 'd-clusters') have been considered as potential candidates for the cooperatively rearranging regions of Adam and Gibbs [18]. A note of caution must be posed here, however. The cooperatively rearranging regions represent theoretically idealized, fixed size regions in the theory of Adam
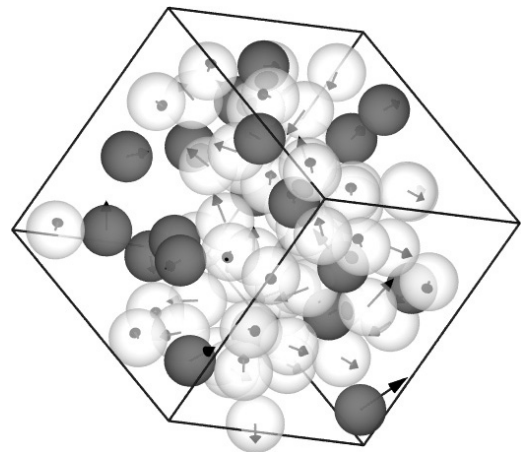

Figure 6. Configuration snapshot of democratic particles (those particles with displacement larger than 0.3 in a 40 time units interval) occurring in the MB–MB transition that starts at $t = 680$ and ends at $t = 720$. The spheres (light and dark for the A and B particles, respectively) give the location of the particles just before the rearrangement and the arrows point to their position right after the transition event. Adapted from [32].

and Gibbs [18]. Calorimetric studies have suggested a size for them to be of around eight molecules close to T_g [50]. This number is clearly very small as compared to the d-cluster sizes.

From the plots shown above, we can easily note that the d-cluster events are fast as compared to t^*, the timescale associated with the string objects. Also evident is the fact that the α relaxation for the system is performed after a few such events (as can be learnt for example from figure 3 where the total timescale corresponds to τ_α). The interesting result is thus that the dynamics is not homogeneous in time, since the trajectory is confined for long times to a certain region of configuration space (thus remaining inactive in terms of the
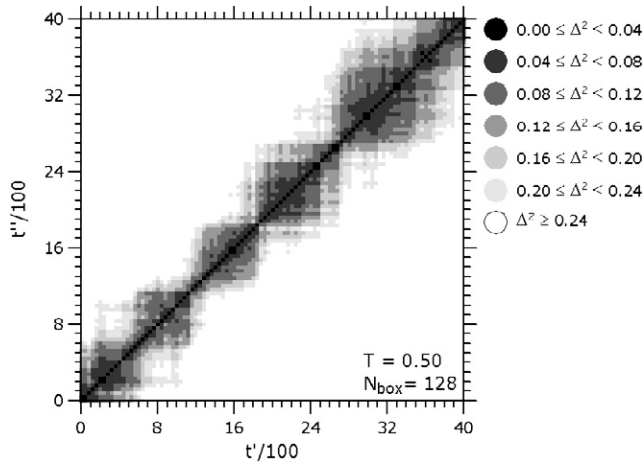
Figure 7. Contour plot of the distance matrix $\Delta^2(t', t'')$ for the binary Lennard-Jones system at $T = 0.50$ within one of the 64 boxes into which the large $N = 8000$ system was divided. The grey levels correspond to the values that are given to the right.

Figure 8. For the trajectory in a small box with $N_{box} = 128$ at $T = 0.50$ (that of figure 7): the function $w(t, t + t^*)$ (vertical bars, left scale), which gives the fraction of mobile particles (those particles with displacements larger than 0.6 in a t^* time interval) and the corresponding $\delta^2(t, \theta)$ (solid line, right scale). The values of t^* and θ are 400 and 160, respectively.

α relaxation) to then suffer rapid bursts of mobility (the d-clusters) that make a significant contribution to the structural relaxation (we also indicate that within an MB one can find some particles with large displacements and also some small strings which are born and die out in isolation without making any significant contribution to the α relaxation).

In turn, the relatively compact nature of the d-clusters would be compatible with the geometrical structure of the dynamic correlations at large timescales of the order of τ_α, as indicated in an inhomogeneous mode-coupling theory (contrary to the less dense structures, compatible with string-like motions, expected at the shorter timescales of the β-relaxation time, a timescale much shorter than that required to exit the plateau in the mean squared displacement and thus, much shorter than τ_α) [17]. The d-clusters are also supposed to be related to the soft modes present in the system at the corresponding time [17, 51, 52]. Additionally, they have also been related to a very appealing description of glassy relaxation known as the dynamic facilitation theory [20, 21]. In this theory, glassiness results from the existence of effective constraints on the dynamics of the system. This approach was first conceived from simple microscopic facilitated spin models such as the Fredrickson–Andersen (FA) [53] and the East model [54]. In one dimension these models are described by a chain of Ising spins $n_i = \{0; 1\}$, with a trivial Hamiltonian $H = \sum_i n_i$, where $n_i = 1$ represents a mobile site or excitation and $n_i = 0$ represents an immobile, or jammed site. Glassiness is the result of local dynamical rules that specify the ability of a site to change state. In the FA model a site can only flip if either of its nearest neighbours is in the excited state, while for the East model a spin may only flip if its nearest neighbour to the left is excited, thus propagating excitations in an eastward direction. Relaxation is Arrhenius in the FA and super-Arrhenius in the East model [20, 21, 55]. At low temperatures the dynamical trajectories are spatially heterogeneous, excitations form continuous lines in space–time, and there are large inactive space–time 'bubbles'. Hedges and Garrahan [55] calculated a distance matrix similar to the
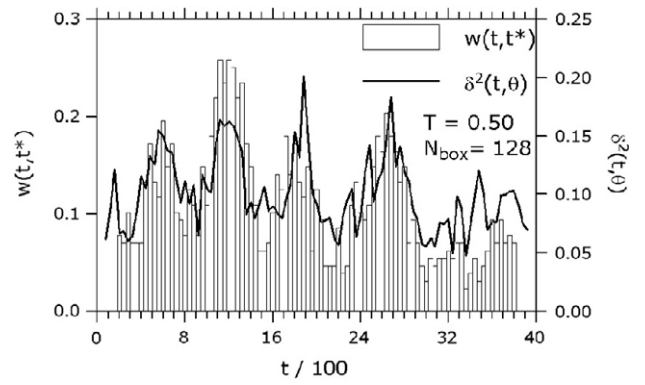
ones we studied before but for the spin facilitated models where the distance between structures was measured in terms of the number of kinks or number of times each site i has changed state between two configurations. An island structure of the distance matrix and sporadic rapid bursts in mobility were found in agreement with our results for binary Lennard-Jones systems. These authors thus indicated that in these systems, the d-clusters were a result of facilitation, with the global relaxation event resulting from a sequence of close locally facilitated steps, and whose size was determined by the extent to which the excitation line penetrated the sub-region (the size of the bubbles). Similar results were also yielded by the two-vacancy assisted triangular lattice gas or (2)-TLG [55].

So far we have only focused on a small system of $N = 150$ particles. To demonstrate that this behaviour is also typical of the different regions of a large system, we now divide a system of $N = 8000$ into 64 adjacent equal-size cubic boxes, so each box has $N_{box} \approx 125$ particles. In order to study the relaxation behaviour of any of such boxes, we tag the particles of the corresponding box at $t = 0$ and apply the above-expounded methods (we do this since in a timescale of length τ_α the particles do not move much, not more than the interparticle distance on average). Since we expect the large system to suffer different d-clusters at different regions of the sample, this method of rigid arbitrarily placed boxes would not be optimal (the d-cluster events need not be entirely contained within a box but should be cut by our arbitrary box boundaries). Thus, we expect that the results will be less neat than for the isolated $N = 150$ particles system (however, we do not expect them to change qualitatively). The behaviour we find for a given box is indeed quite similar to that previously expounded for the isolated system of $N = 150$, as can be learnt from figures 7–10.

Figure 7 displays the distance matrix for the trajectory evaluated within one such small box, while figure 8 exhibits the corresponding $\delta^2(t, \theta)$ for $\theta = 160$ (solid line, right scale). Both plots speak of a metabasin structure and signal the presence of d-clusters. If we now look at any other box
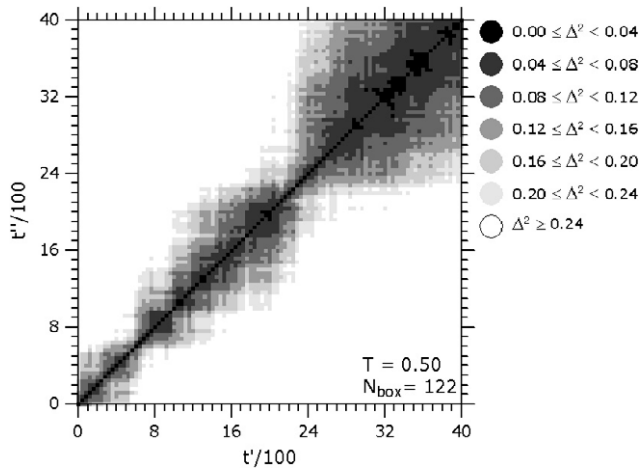
Figure 9. Contour plot of the distance matrix $\Delta^2(t', t'')$ for the binary Lennard-Jones system at $T = 0.50$ within one of the 64 boxes (non-adjacent to the one of figure 7) into which the large $N = 8000$ system was divided. The grey levels correspond to the values that are given to the right.
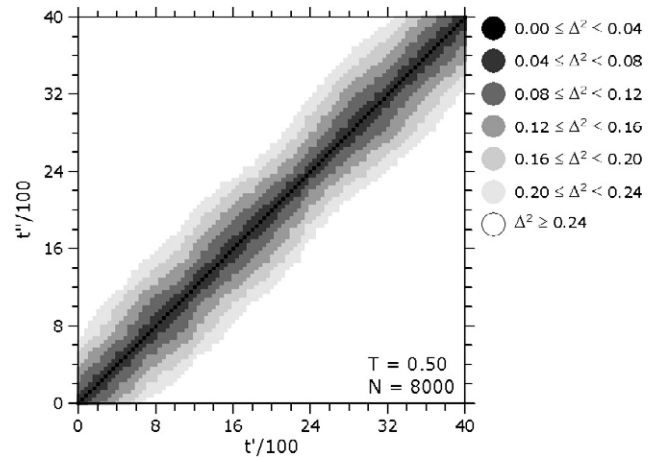

Figure 11. Typical contour plot of the distance matrix $\Delta^2(t', t'')$ for the binary Lennard-Jones system at $T = 0.50$ and $N = 8000$. The grey levels correspond to the values that are given to the right.
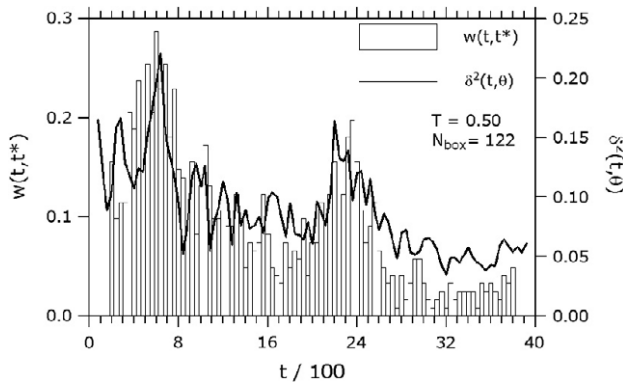

Figure 10. For the trajectory in a small box with $N_{\text{box}} = 122$ at $T = 0.50$ (that of figure 9). The function $w(t, t + t^*)$ (vertical bars, left scale), which gives the fraction of mobile particles (those particles with displacements larger than 0.6 in a t^* time interval) and the corresponding $\delta^2(t, \theta)$ (solid line, right scale). The values of t^* and θ are 400 and 160, respectively.
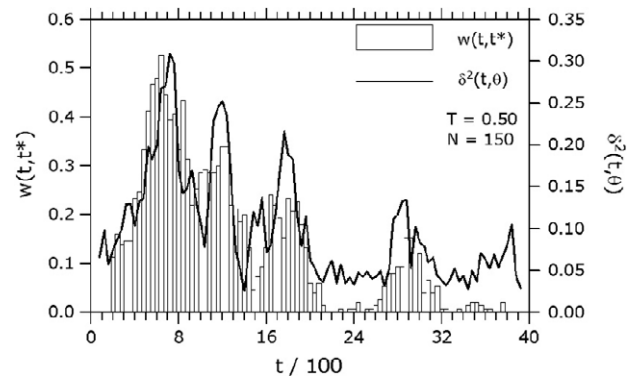

Figure 12. For the trajectory given in figure 4 for the binary Lennard-Jones system of $N = 150$ at $T = 0.50$: the fraction of mobile particles $w(t, t^*)$ within the time interval $[t - t^*/2, t + t^*/2]$ (vertical bars, left scale) and the corresponding $\delta^2(t, \theta)$ (solid line, right scale). The values of t^* and θ are 400 and 160, respectively.

for the same trajectory (the same times and within the same large system), we get a similar distance matrix structure and the presence of d-clusters. This can be seen in figures 9 and 10 for another box (not adjacent to the previous one).

However, the times at which the d-clusters and MB–MB transitions occur differ from the ones of the previous box and also from the ones of other boxes. This implies that (spatially) averaging over the different regions washes out the heterogeneity and thus the dynamics for a large system should look homogeneous in time (in figure 11 we show the distance matrix for the full system of $N = 8000$ which gives a dark main diagonal fading out as we move away from it, thus lacking the square-like island structure present for small boxes). This means that in a large system different regions would be 'active' (present d-clusters) at different times, as was the case when we studied the time evolution of the occurrence of the different strings in a system of $N = 500$ [38].

This moves one to think that, even when the nature of both kinds of objects (d-clusters and mobile/string clusters) is quite different, there should be a relationship between them. Focusing on a small box of a large system (or if we work with an isolated small system) and considering a t^* length timescale, we expect that if the system presents a d-cluster at any time within such a time interval then the two-snapshot ($t = 0$ and t^*) analysis of [12–14] would find many mobile particles and even string-like clusters. Thus, to demonstrate the relationship between both approaches we have calculated (for the same trajectories previously analysed of the system of $N = 150$ and for the two small boxes within the large system of $N = 8000$) the fraction of mobile particles with the same mobility criterion as [12–14]. However, instead of focusing on a fixed time interval, we calculate such a quantity as a function of time. That is, a mobile particle at time t is that for which $|\mathbf{r}_i(t + t^*/2) - \mathbf{r}_i(t - t^*/2)| > 0.6$. We name the fraction of such particles within the considered small system/box at time t as $w(t, t^*)$. In figure 12 we show a plot of such a function for the same trajectory previously studied for the system of $N = 150$
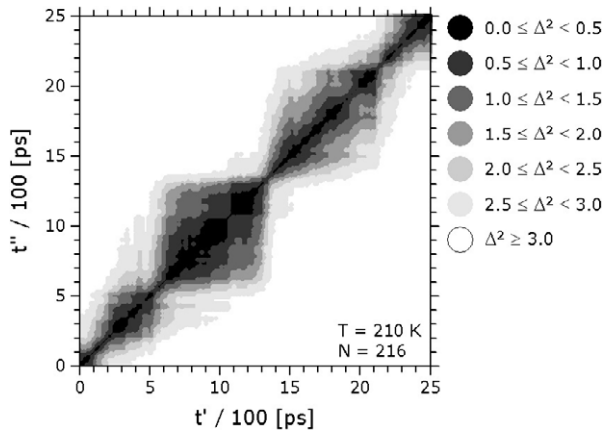
Figure 13. Contour plot of the distance matrix $\Delta^2(t', t'')$ for a system of $N = 216$ water molecules interacting via the SPC/E potential at $T = 210$ K. The grey level corresponds to values of $\Delta^2(t', t'')$ that are given to the right of the figure (units are Å^2). Adapted from [61].

Figure 14. Solid line (right scale): average squared displacement $\delta^2(t, \theta)$ for the trajectory given in figure 13. The value of θ is 40 ps. Vertical bars (left scale): the function $m(t, \phi)$ which gives the fraction of oxygen atoms that moved more than the threshold value $r_{th} = 0.06$ nm in the time interval $[t, t + \phi]$, using $\phi = 10$ ps. Adapted from [61].

together with δ^2 (as given in figure 4), a function that we have already seen that signals the presence of d-clusters. The average of $w(t, t^*)$ in time should yield an equivalent value as its average over a large system (here this value is around 14%). We can see that $w(t, t^*)$ presents important peaks that coincide nicely with that of the δ^2. This implies a strong relationship between the mobile clusters of [12–14] and the d-clusters. This is also the case for the two small boxes within the large system, as can be learnt from the vertical bars (left scale) from figures 8 and 10.

5. d-clusters beyond Lennard-Jones

5.1. d-clusters in supercooled amorphous water

At this point it seems worth wondering whether the d-clusters are particular features of the dynamics of the simple binary Lennard-Jones system or if they also emerge in the relaxation dynamics of more complex, realistic systems. Thus, we shall now focus on another glass former, namely supercooled amorphous water. From a dynamical viewpoint, it has been shown computationally that supercooled amorphous water confirms the general picture of dynamical heterogeneities [56–59], with mobile molecules arranged in clusters usually linked by hydrogen bonds. The properties of its potential energy landscape have also been studied, including the characterization of transitions between ISs [57]. Here we shall show the results obtained for a system of $N = 216$ water molecules interacting via the simple point charge extended (SPC/E) model [60] in the NVE ensemble [61] (the integration step was 1 fs and long-range interactions were taken into account using the reaction field method). At temperatures within the supercooled regime both the real dynamics (the instantaneous MD structures) and the inherent dynamics (the ISs of the corresponding instantaneous structures, calculated by performing a minimization of the energy of these instantaneous structures using a standard conjugate gradient minimization algorithm [62]) were investigated. In order to
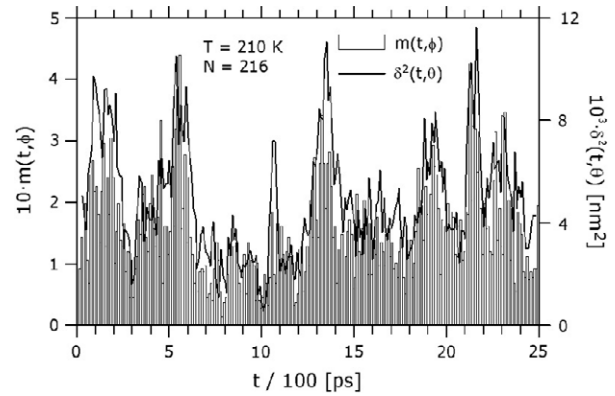
study the possible MB structure of this system a number of 250 configurations were recorded at fixed time intervals of 10 ps—at density 1 g cm^{-3} and $T = 210$ K. We note that the total run time was larger than the α-relaxation time and that the behaviour obtained at other close temperatures was similar. Also, similar results were found by directly using the instantaneous structures instead of the ISs.

Figure 13 shows typical results [61] for a run at $T = 210$ K when the distance matrix approach is used as in the case of the binary Lennard-Jones (focusing on the positions of the oxygen atoms of the water molecules in the ISs). The grey level of the squares in the $\Delta^2(t', t'')$ depicts the (average squared) distance between the corresponding configurations at times t' and t'', the darker the shading indicating the lower the distance between them. From the island structure of this matrix we can learn that a clear MB structure of the landscape is also evident here, as was the case for the Lennard-Jones systems. In turn, figure 14 shows the time evolution of the average squared displacement $\delta^2(t, \theta)$ in the time interval $\theta = 40$ ps (solid line, right scale) [61].

The vertical bars (left scale) of figure 14 display the function $m(t, \phi)$ [61], which represents the fraction of molecules that have moved more than a threshold value of 0.06 nm in time intervals $[t, t + \phi]$ with $\phi = 10$ ps (we note that an integration of the self part of the van Hove function, $4\pi r^2 G_s(r, \phi)$, from 0.06 to infinity gives less than 0.15 and that similar results arise for other threshold values). Thus, in agreement with the previous findings for binary Lennard-Jones systems, MB–MB transitions imply the rearrangement of a substantial number of the molecules of the system. That is, these results clearly demonstrate that also for supercooled amorphous water the α-relaxation time corresponds to a small number of crossings from one MB to a neighbouring one, each crossing being very rapid and involving the collective motion of a great number of molecules. From direct inspection of the function $m(t, \phi)$ in figure 14 we can see that in the MB–MB transitions 35%–45% of the molecules move more than 0.06 nm in 10 ps, a time span slightly larger than 1% τ_α.
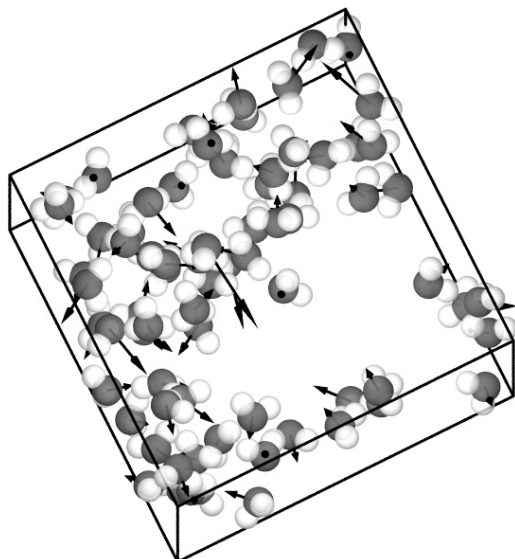
Figure 15. Configuration snapshot of democratic molecules occurring in the MB–MB transition $t = 1320$–1330 ps. The spheres (light and dark for the hydrogen and oxygen atoms, respectively) give the location of the atoms of the water molecule before the rearrangement and the arrows point to the position of the oxygen atom after the transition (to help visualize the particle movements, the arrows are twice the length of the corresponding displacement vector). Adapted from [61].

Additionally, it can be noted that the events that constitute the local exploration of the MB do not contribute to the structural relaxation of the system. Thus, these results demonstrate the prevailing role of MB–MB transitions for the long-time dynamics.

Figure 15 shows a three-dimensional plot of the democratic molecules (mobility greater than 0.06 nm in a 10 ps time window) for one of the time intervals of figure 14, namely that which goes from $t = 1320$ to 1330 ps, but similar results were found for other MB–MB transitions [61]. We show each democratic water molecule (the oxygens and the hydrogens) indicating the position at $t = 1320$ ps and attaching a vector that indicates their displacement to the position occupied at time $t = 1330$ ps (for practical reasons, the modulus of each vector is twice its actual value). A clear cluster arrangement is evident from such a picture with democratic molecules located close to the borders of the simulation box and an empty space at the centre (the molecules in such a region are not democratic). Thus, relatively compact clusters of molecules conforming cooperative relaxing units (the d-clusters found previously for the Lennard-Jones systems) also emerge here as being responsible for the structural relaxation of the system. Additionally, it has been shown that there is a connection between these clusters and local structural 'defects' [61] such as highly coordinated water molecules (more than four first neighbours within a sphere of size 0.30 nm) and bifurcated hydrogen bonds (where one hydrogen of a molecule is bonded to two water molecules instead of a single one), effects that had previously been regarded as mobility promoters [57, 63, 64].

In addition to the above alluded results on the role of d-clusters in binary Lennard-Jones and water, we also would like

to note that we have unpublished evidence for the fast MB–MB transition events and d-clusters in liquid silica interacting via the BKS (van Beest, Kramer and van Santen) model [65]. Thus, these events do not seem to depend on specific detail but to emerge in glass formers quite different in nature.

5.2. Experimental evidences

The question that remains is whether the d-clusters appear merely in the computer simulations or whether experimental evidence can be found for their existence. A complete review of the experimental detection of dynamical heterogeneities has been provided by Richert [11]. It is interesting to note that nuclear magnetic resonance (NMR) studies of supercooled propylene carbonate [66] have shown the α relaxation to be a mixture of many frequent smooth rotational movements (small-angle jumps) and a few large-angle jumps. Thus, in addition to simple rotational diffusion, the α relaxation implies the existence of sporadic translational movements. This finding of infrequent translational jumps could be consistent with the d-cluster description. However, we note that the above described quantities (average squared displacement, $\delta^2(t, \theta)$, distance matrix, $\Delta^2(t', t'')$, etc) were calculated in our simulations in such a way that they are only sensitive to translational diffusion and thus rotational diffusion is not considered (an interesting computational study of rotational diffusion on the rigid three-site model of the fragile glass former ortho-terphenil has been performed [67], where also the decoupling [11, 68] between translational and rotational diffusion was considered).

However, most of the experimental techniques sample ensemble-averaged quantities. In this sense, for a more direct comparison with our simulation results we must resort to microscopic techniques. In this context, as already mentioned, 3D time-resolved confocal spectroscopy has been used in colloidal systems [35, 36]. The position of many particles could be tracked as a function of time (at very short-time spans) and clusters of mobile particles could be identified. While these clusters could be compatible both with the string and the d-cluster descriptions, the time span chosen to define mobile particles (the timescale of maximum inhomogeneous behaviour, t^*, and thus the use of only two snapshots of the configurations of the particles separated at t^* time) prevents us from comparing the results with the fast d-cluster events that trigger the MB–MB transitions. However, we note that the complete set of data of such a study (the configurations of the particles at a number of intermediate times) could be used to calculate functions such as the average squared displacement, $\delta^2(t, \theta)$, and the distance matrix, $\Delta^2(t', t'')$, between others and thus directly probe the validity of the d-cluster description (a task we consider would be worth performing in the future).

In any case, colloidal suspensions are also (experimental) idealized models. Studies on more realistic molecular systems would also be necessary. In this sense, a very nice study of a polymeric system by means of single molecule confocal spectroscopy (which constitutes a test of the MB–MB transitions and d-clusters scenario) has been recently performed [69, 70]. Using single molecule spectroscopy it

was shown [69, 70] that the fluorescence lifetime trajectories of single probe molecules embedded (at high dilution) in a glass-forming polymer melt exhibit strong fluctuations of a hopping character, features that are never present in a polymer melt in thermal equilibrium nor in a polymer in the frozen glassy state. The plausible conclusion of these experimental studies was that this hopping behaviour should be linked to the anomalous features of relaxation phenomena expected to occur in deeply supercooled fluids, dynamical heterogeneity, rugged potential energy landscape, cooperatively rearranging regions, etc. Using MD simulations targeted to explain these experimental observations [69, 70], these authors showed that these lifetime fluctuations correlate strongly with the average square displacement function δ^2 of the polymer matrix. As the dynamics of the probe follows that of the polymer, the latter observable can represent a direct test for the metabasin transitions in the potential energy landscape of this glass-forming polymer matrix. The experiment was carried out using several types of fluorescent probes (differing in their size and/or mass within reasonable limits) embedded in a (glass-forming) polymer matrix of low molar mass of oligo(styrene) above its glass-transition temperature. Along with this, MD NVE simulations of a system containing 120 bead-spring chains of 10 effective monomers were performed. The mass and the size of the beads in the dumbbell were, of course, chosen in order to fit the experimental conditions. The interaction between the two beads of the probe or monomers was given by a Lennard-Jones potential. It was found that the dynamics of the probe follows that of the surrounding polymer, as measured by the self-intermediate scattering function. Furthermore, the latter is not disturbed by the presence of the fluorescent probe. Applying the distance matrix method to the polymeric matrix, they showed that its dynamics is very heterogeneous in time, staying for a relatively long time close to one region (MB) in its configuration space prior to a jump to another region. Furthermore, the jumps in the fluorescence lifetime trajectory correlated with the MB–MB transitions observed at the crossings between successive MBs. To show this correlation quantitatively, they calculated the $\delta^2(t, \theta)$ (the same function we used above) of the monomers within a time interval chosen to be 4% of the relaxation time [69]. One then can see that each jump of the fluorescence is accompanied by a maximum of the $\delta^2(t, \theta)$ function and can thus signal an MB–MB transition. Additionally, they obtained a distance matrix plot that resembles very much the ones we have presented above for the binary Lennard-Jones and water. Thus, these mixed experimental-computational studies in a glassy polymer show a clear accord with our computational results in binary Lennard-Jones systems and SPC/E water. We can then expect that the appearance of the same kind of behaviour in systems that are microscopically very different would speak of the generality of the d-cluster MB–MB transitions picture in the context of glassy relaxation.

6. Relationship of d-clusters to local structure

In the former sections we have established the relevance of the d-cluster events to the α-relaxation dynamics of glass-forming systems. However, not much has been said about

structural facts. We intuitively expect the d-clusters or 'active' regions to be indeed related to structural heterogeneities in the sample (regions more 'unblocked' or 'unjammed'). However, the determination of the existence of a causal link between structure and dynamics remains another major unsolved problem in the field [2, 71, 72].

A recent breakthrough in this context [72, 71] was the introduction of the isoconfigurational ensemble (IC). In it one performs a series of equal length MD trajectories from the same initial configuration, that is, always the same structure (the same particle positions) but each trajectory having different initial particle momenta chosen at random from the appropriate Maxwell–Boltzmann velocity distribution.

Propensity of a particle i to move in the initial configuration ($t = 0$) for a time ξ from $t = 0$, was defined as $\langle \Delta \mathbf{r}_i^2 \rangle_{\mathrm{IC}}$ [71], where $\Delta \mathbf{r}_i^2 = |\mathbf{r}_i(\xi) - \mathbf{r}_i(0)|^2$ is the quadratic displacement of particle i in the time interval $[0, \xi]$ for each trajectory of the IC and $\langle \cdots \rangle_{\mathrm{IC}}$ is the average over such an IC. Therefore, for 2D soft disks this definition allowed to determine that at low temperatures the propensity for motion of the particles from any given configuration for a time ξ is not uniform throughout the sample and high propensity particles are confined to certain (relatively compact) regions [71] This result also holds for the binary Lennard-Jones system here under study [74]. Thus, while particle mobility is not reproducible from trajectory to trajectory, the spatial variation in the propensity is completely determined by the initial configuration, reflecting the influence of structure on dynamics [71, 74]. A propensity much greater than its mean value, a great tendency to be mobile, is thus a clear indication that the particle is not 'comfortable' in its present position, that is, it is structurally unjammed.

Thus, it became of great interest to explore the connections between high propensity regions and d-clusters. In so doing, we found that the high propensity regions of a given initial configuration represent unblocked zones wherein d-clusters occur in the subsequent dynamics (for any given IC realization or trajectory initiated in such a configuration) [73]. In turn, the reciprocal is also valid: the occurrence of a d-cluster reformulates the propensity regions of the sample [74, 75]. An interesting result is that the influence of the local structure on the dynamics for the binary Lennard-Jones system does not extend to long times but is on the order of the MB average residence time, a timescale shorter than the α-relaxation time τ_α. Thus the local structural constraints do not survive a d-cluster or MB–MB transition [74]. This was carried out by using an extension of the original definition of the propensity in the form of a time-dependent propensity [74], as we shall see in section 6.1. After doing that, we shall make use of another approach to evidence the role of d-clusters in propensity decorrelation [75].

6.1. The isoconfigurational method. Role of the local structure: time-dependent propensity

To calculate the time-dependent propensity for motion we use a generalization of the IC method introduced in [71] since we are interested in studying how propensity evolves with time within
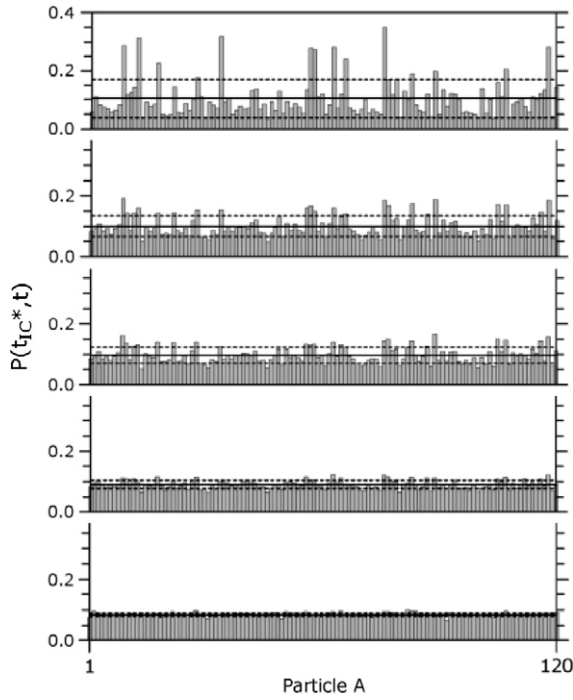
Figure 16. Time-dependent propensity $P(t_{IC}^*, t)$ for the A particles of the $N = 150$ Lennard-Jones system at $T = 0.50$. From top to bottom: $t = 0$; $t = 0.5t_{IC}^*$; $t = t_{IC}^*$; $t = 3t_{IC}^*$ and $t = 9t_{IC}^*$. Solid horizontal lines correspond to average time-dependent propensities $\langle P(t_{IC}^*, t) \rangle$. Dashed horizontal lines indicate $\langle P(t_{IC}^*, t) \rangle \pm \sigma(t_{IC}^*, t)$, where $\sigma(t_{IC}^*, t)$ is the standard deviation.

an IC. Propensity of a particle i for motion in the configuration at time t (its tendency to be mobile at the instantaneous time t on the given trajectory) for a fixed time interval of length t^* is defined as $P_i(t_{IC}^*, t) = \langle |\mathbf{r}_i(t + t_{IC}^*) - \mathbf{r}_i(t)|^2 \rangle_{IC}$, where $\langle \cdots \rangle_{IC}$ indicates an average over the IC generated at time $t = 0$ and t_{IC}^* is the t^* averaged over the different trajectories over the IC. This procedure allows us to study the persistence of the 'memory' in the propensity calculated from the initial structure ($t = 0$). We note that the average time-dependent propensity $\langle P(t_{IC}^*, t) \rangle = N^{-1} \sum_i^N P_i(t_{IC}^*, t)$ is approximately constant as a function of t. However, the dispersion in the propensity values falls quickly, within a timescale close to t_{IC}^*. This can be seen in figure 16. In the case of $P(t_{IC}^*, 0)$ (the curve at the top), there are A particles with very high and also very low time-dependent propensity values (high and low vertical bars), that is, great fluctuations from the mean value. However, at larger times, the time-dependent propensities of the different particles become uniform, that is, they do not differ much from the mean value. These results speak of a rapid loss of the influence of the initial structural constraints.

At first all the trajectories (within an IC) are confined to the same local MB (in which is located the initial structure that generates the IC), wherein each of them resides for different amounts of time before escaping by means of a different d-cluster [74]. Thus, there exists a distribution of residence times in the local MB (some of the trajectories being able to abandon the MB at very short times while others have to spend large times). Thus, a single trajectory is not able to determine the

confining nature of a given MB. In this regard, it has been found that at any given T different ICs present local MBs with different confining properties, and the mean residence time for the local MB in an IC is very close to the t_{IC}^* (evaluated in the corresponding IC) [74]. In turn, the different trajectories (over an IC) that at first were confined to the same local MB leave to different second MBs, since there is a large multiplicity of neighbouring MBs. Thus, the propensity de-correlates after the first MB–MB transition [74]. This result also supports the validity of a random-walk scenario (spatially uncorrelated hopping processes between MBs) for the long-time diffusion of glassy systems [74, 47, 26].

6.2. Role of d-clusters in propensity de-correlation

To elucidate the role of the d-clusters in reformulating the local structural constraints it is useful to start many ICs *over* a given single dynamical trajectory [75]. Here we show such an approach for the same MD run of figures 3–5 (that is, for the isolated small $N = 150$ system at $T = 0.50$). We recorded a configuration every 40 time units (a total of 101 configurations, for a total length of $\tau_\alpha = 4000$) and generated for each of them an IC. Thus, we determined the propensities for each of the 101 equally spaced initial configurations over the given MD trajectory. The way the spatial distribution of propensity (the value of the propensity for each particle) changes from one (initial) configuration to another (from one IC to another), gives an idea of the time evolution of the local structural constraints.

To quantify how similar or different is the propensity of the different particles in configurations at times t' and t'' (over the trajectory of figures 3–5), we calculate the following cross-correlation function $R(t', t'') = \sum_{i=1}^{N_{box}} R_i$, where:

$$R_i = \frac{[X_i - \langle X \rangle]}{\{\sum_{l=1}^{N_{box}} [X_l - \langle X \rangle]^2\}^{1/2}} \frac{[Y_i - \langle Y \rangle]}{\{\sum_{l=1}^{N_{box}} [Y_l - \langle Y \rangle]^2\}^{1/2}}.$$

In it, X_i and Y_i are respectively $P_i^\dagger(\xi, t')$ and $P_i^\dagger(\xi, t'')$. $P_i^\dagger(\xi, t)$ is the propensity of particle i calculated over the IC generated from the configuration (in the trajectory in figures 3–5) at time t. Each of these ICs entangle 500 trajectories of total run length $\xi = 40$ time units[4]. Besides $\langle X \rangle$ and $\langle Y \rangle$ are respectively $\langle P^\dagger(\xi, t') \rangle$ and $\langle P^\dagger(\xi, t'') \rangle$, where $\langle P^\dagger(\xi, t) \rangle = N^{-1} \sum_{i=1}^N P_i^\dagger(\xi, t)$. Basically, $R(t', t'') = 1$ indicates that $P_i^\dagger(\xi, t') = P_i^\dagger(\xi, t'')$, while values of $R(t', t'')$ close to zero indicate that the propensity of particle i has changed significantly between t' and t''. Figure 17 depicts $R(t', t'')$. We recall that such a function is built upon 'structural information' while $\Delta^2(t', t'')$ of figure 3 relies on dynamical data. $R(t', t'')$ is based on the propensity for motion of the particles calculated at very short time intervals $\xi = 40$ (at times t' and t'') and thus reflects the cross-correlations between the local structural constraints of the configurations at these corresponding times.

---

[4] While the mean value of the propensity [$\langle P^\dagger(\xi, t) \rangle = N^{-1} \sum_{i=1}^N P_i^\dagger(\xi, t)$] depends on the time length ξ in which it is calculated, the spatial variation of propensity does not depend on it for times not too small (down to 10% t^* or even less) [76, 72]. In other words, if one calculates the propensity at $\xi = t^*$ or somewhat higher or if one does it for a timescale of 10% t^*, the particles with higher and lower propensity are the same in any case.
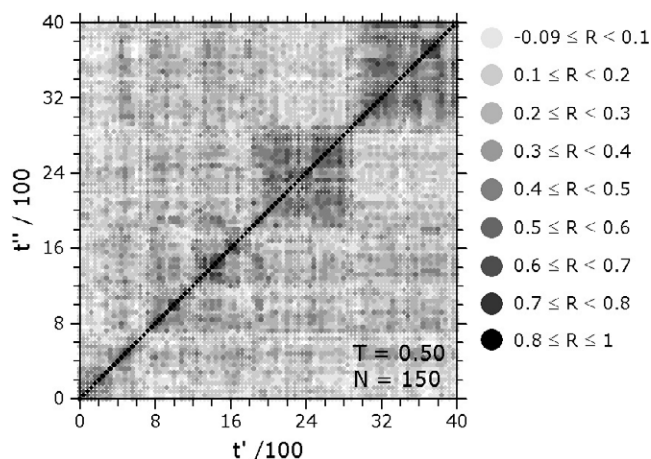
Figure 17. Cross-correlation function $R(t', t'')$ between propensities calculated over ICs generated from configurations at times t' and t'' that belong to the trajectory for the system of $N = 150$ given in figure 3. The propensities, in the corresponding IC at time t, are calculated among 500 trajectories for a $\xi = 40$ time interval. The grey levels correspond to the values that are given to the right.

We also note that if we calculate propensities at larger times (say, for example at $\xi = t^*$ instead of $\xi = 40$), the results are consistent, and even more conspicuous. Direct inspection of the propensity–propensity cross-correlation matrix R of figure 17 evidences a structure which matches very well that of the MBs of figure 3. We can see that large values of R (dark regions) occur at times when figure 3 shows a metabasin structure. This means that the propensity of the particles within an MB are positively correlated, that is to say, the propensity of each particle is similar in all the corresponding ICs. Since R is generally small for ICs not belonging to the same MB (grey regions), the propensity of the particles at such times does not present a neat correlation. Moreover, the borders of the square islands of figure 17 show certain small negative values, thus indicating a slight anti-correlation in propensity once the system abandons the local MB (high propensity particles change to low propensity, or intermediate propensity, and vice versa). This fact means that the propensity de-correlates after an MB–MB transition and thus, that the d-clusters reformulate the propensity pattern by rearranging the regions of high, medium and low propensity (a fact also consistent with a rapid loss of the memory of the local structure, that is, of the structural constraints of the present MB, once a trajectory of the system escapes from this MB). To summarize, the above results make evident the interplay between structure and dynamics: d-clusters relax the high propensity regions to generate new distinct 'unblocked' domains and vice versa.

7. Conclusions

In this work we have reviewed the molecular events involved in the relaxation dynamics of glass-forming systems in the supercooled regime. We have put special emphasis on the events characteristic of the dynamical heterogeneities. First, we described the cooperative events responsible for the departure of the dynamics from a Gaussian behaviour:

structurally open-like clusters of mobile particles including string-like motions. However, when focusing on the structural or α relaxation, we have described the dominant role of democratic clusters (d-clusters), events that trigger the transition between metabasins of the potential energy landscape of the system. We have shown that the d-clusters are in fact related to the mobile particles that form the more open-like clusters (strings) previously described, but that are the first ones unambiguously related to the long-time structural relaxation and that they provide a more complete picture of this process. Such a picture reveals the fact that the dynamics of each of the different regions of the system is not only heterogeneous *in space* but also *in time*, since the trajectory is confined for long times to a certain portion of configuration space (metabasin) to then cross to another different one. These crossings entail the emergence of cooperatively relaxing units in the form of relatively compact clusters built up by a significant portion of the particles within the corresponding region (d-cluster), an event that occurs in the form of a burst of mobility. Such sporadic rapid motions are the main factors responsible for the α relaxation, which is completed after a few such events, since the events related to the exploration of the local MB do not contribute appreciably. We have also provided arguments for the generality of such a scenario, since we have shown that the d-clusters arise in systems very different in nature such as a binary Lennard-Jones system (simple model glass former) and supercooled amorphous water and that they have received experimental support from a single molecule technique in a glassy polymer. Additionally, we have also related such events to the dynamic propensity (the tendency of the particles to be mobile in a given structure) of the different regions of the sample, a description that signals the existence of a link between the local structure and the corresponding dynamics. In this context, we have shown the role of the d-clusters in the loss of the memory the system experiences from its initial structure by reformulating the mobility tendency of the different regions of the sample, thus elucidating the existence of a mutual transfer of constraints between local structure and dynamics.

13

References

[1] Angell C A 1991 *J. Non-Cryst. Solids* **131** 13
[2] Ediger M D 2000 *Annu. Rev. Phys. Chem.* **51** 99
[3] Debenedetti P G and Stillinger F H 2001 *Nature* **410** 259
[4] Ediger M D, Angell C A and Nagel S R 1996 *J. Phys. Chem.* B **100** 13200
[5] Götze W 1999 *J. Phys.: Condens. Matter* **11** A1
[6] Ngai K L, Floudas G, Rizos A K and Riande E (ed) 2002 *Proc. 4th Int. Discussion Mtg on Relaxations in Complex Systems (Heraklion, Crete, June 2001) J. Non-Cryst. Solids* **307–10** Special issues
[7] Debenedetti P G 1996 *Metastable Liquids: Concepts and Principles* (Princeton, NJ: Princeton University Press)
[8] Binder K and Kob W 2005 *Glassy Materials and Disordered Solids: an Introduction to their Statistical Mechanics* (Singapore: World Scientific)
[9] Cicerone M T, Blackburn F R and Ediger M D 1995 *J. Chem. Phys.* **102** 471
[10] Schmidt-Rohr K and Spiess H W 1991 *Phys. Rev. Lett.* **66** 3020
[11] Richert R 2002 *J. Phys.: Condens. Matter* **12** R703
[12] Kob K, Donati C, Plimpton S J, Poole P H and Glotzer S C 1997 *Phys. Rev. Lett.* **79** 2827
[13] Donati C, Douglas J F, Kob W, Plimpton S J, Poole P H and Glotzer S C 1998 *Phys. Rev. Lett.* **80** 2338
[14] Donati C, Glotzer S C, Poole P H, Kob W and Plimpton S J 1999 *Phys. Rev.* E **60** 3107
[15] Kob W 1999 *J. Phys.: Condens. Matter* **11** R85
[16] Götze W and Sjogren L 1992 *Rep. Prog. Phys.* **55** 241
[17] Biroli G, Bouchaud J-P, Miyazaki K and Reichman D 2006 *Phys. Rev. Lett.* **97** 195701
[18] Adam G and Gibbs J H 1965 *J. Chem. Phys.* **43** 139
[19] Kirkpatrick T R, Thirumalai D and Wolynes P G 1989 *Phys. Rev.* A **40** 1045
[20] Garrahan J P and Chandler D 2002 *Phys. Rev. Lett.* **89** 035704
[21] Garrahan J P and Chandler D 2003 *Proc. Natl Acad. Sci. USA* **100** 9710
[22] Xia X and Wolynes P G 2001 *Phys. Rev. Lett.* **86** 5526
[23] Cavagna A, Grigera T and Verrocchio P 2007 *Phys. Rev. Lett.* **98** 187801
[24] Tarjus G and Kivelson D 1995 *J. Chem. Phys.* **103** 3071
[25] Ngai K L 2005 *J. Non-Cryst. Solids* **351** 2635
[26] Heuer A 2008 *J. Phys.: Condens. Matter* **20** 373101
[27] Dyre J C 2006 *Rev. Mod. Phys.* **78** 953
[28] Lubchenko V and Wolynes P G 2007 *Annu. Rev. Phys. Chem.* **58** 235
[29] Kob W and Andersen H C 1994 *Phys. Rev. Lett.* **73** 1376
[30] Kob W and Andersen H C 1995 *Phys. Rev.* E **51** 4626
[31] Kob W and Andersen H C 1995 *Phys. Rev.* 52 4134
[32] Appignanesi G A, Rodriguez Fris J A, Montani R A and Kob W 2006 *Phys. Rev. Lett.* **96** 057801
[33] Rahman A 1964 *Phys. Rev.* **136** A405
[34] Hansen J-P and McDonald I R 1986 *Theory of Simple Liquids* (London: Academic)
[35] Weeks E R, Crocker J C, Levitt A C, Schofield A and Weitz D A 2000 *Science* **287** 627
[36] Kegel W K and van Blaaderen A 2000 *Science* **287** 290
[37] Appignanesi G A, Frechero M A and Montani R A 2003 *Physica* A **329** 41
[38] Appignanesi G A, Frechero M A, Alarcón L M, Rodriguez Fris J A and Montani R A 2004 *Physica* A **339** 469
[39] Ohmine I 1995 *J. Phys. Chem.* **99** 6765
[40] Wales D J 2003 *Energy Landscapes* (Cambridge: Cambridge University Press)
[41] Sciortino F 2005 *J. Stat. Mech.* P05015
[42] Goldstein M 1969 *J. Chem. Phys.* **51** 3728
[43] Stillinger F H and Weber T A 1982 *Phys. Rev.* A **25** 978
[44] Stillinger F H and Weber T A 1984 *Science* **225** 983
[45] Stillinger F H 1995 *Science* **267** 1935
[46] Sastry S, Debenedetti P G and Stillinger F H 1998 *Nature* **393** 554
[47] Doliwa B and Heuer A 2003 *Phys. Rev.* E **67** 031506
[48] Heuer A 1997 *Phys. Rev. Lett.* **78** 4051
[49] Vogel M, Doliwa B, Heuer A and Glotzer S C 2004 *J. Chem. Phys.* **120** 4404
[50] Yamamuro O *et al* 1998 *J. Phys. Chem.* B **102** 1605
[51] Brito C and Wyart M 2007 *J. Stat. Mech.* L08003
[52] Coslovich D and Pastore G 2007 *J. Chem. Phys.* **127** 124505
[53] Fredrickson G H and Andersen H C 1984 *Phys. Rev. Lett.* **53** 1244
[54] Jäckle J and Eisinger S 1991 *Z. Phys.* B **84** 115
[55] Hedges L O and Garrahan J P 2008 *J. Physique* A **41** 3244006
[56] Sciortino F, Gallo P, Tartaglia P and Chen S-H 1996 *Phys. Rev.* E **54** 6331
[57] Giovambattista N, Starr F W, Sciortino F, Buldyrev S V and Stanley H E 2002 *Phys. Rev.* E **65** 041502
[58] Giovambattista N, Buldyrev S V, Starr F W and Stanley H E 2003 *Phys. Rev. Lett.* **90** 085506
[59] Matharoo G S, Gulam Razul M S and Poole P H 2006 *Phys. Rev.* E **74** 050502(R)
[60] Berendsen H J C, Grigera J R and Stroatsma T P 1987 *J. Phys. Chem.* **91** 6269
[61] Rodriguez Fris J A, Appignanesi G A, La Nave E and Sciortino F 2007 *Phys. Rev.* E **75** 041501
[62] Press W H, Flannery B P, Teukolsky S A and Vetterling W T 1986 *Numerical Recipes* (Cambridge: Cambridge University Press)
[63] Sciortino F, Geiger A and Stanley H E 1992 *J. Chem. Phys.* **96** 3857
[64] Sciortino F, Geiger A and Stanley H E 1990 *Phys. Rev. Lett.* **65** 3452
[65] Rodriguez Fris J A, Appignanesi G A and Kob W 2009 in preparation
[66] Qi F *et al* 2000 *J. Chem. Phys.* **112** 9455
[67] Lombardo T G, Debenedetti P G and Stillinger F H 2006 *J. Chem. Phys.* **125** 174507
[68] Stillinger F H and Hodgdon J A 1994 *Phys. Rev.* E **50** 2064
[69] Vallée R A L, van der Auweraer M, Paul W and Binder K 2006 *Phys. Rev. Lett.* **97** 217801
[70] Vallée R A L, Paul W and Binder K 2007 *J. Chem. Phys.* **127** 154903
[71] Widmer-Cooper A, Harrowell P and Fynewever H 2004 *Phys. Rev. Lett.* **93** 135701
[72] Widmer-Cooper A and Harrowell P 2007 *J. Chem. Phys.* **126** 154503
[73] Frechero M A, Alarcón L M, Schulz E P and Appignanesi G A 2006 *Phys. Rev.* E **75** 0110502
[74] Appignanesi G A, Rodriguez Fris J A and Frechero M A 2006 *Phys. Rev. Lett.* **96** 237803
[75] Rodriguez Fris J A, Alarcón L M and Appignanesi G A 2009 *J. Chem. Phys.* **130** 024108
[76] Rodriguez Fris J A, Alarcón L M and Appignanesi G A 2007 *Phys. Rev.* E **76** 011502